"Machining of Advanced Ceramics"

Yoshio TANAKA

1. Introduction

Advanced ceramics have excellent thermal resistance, wear resistance, corrosion resistance, and other properties, and are promising materials as structural materials. Over the past decade, they have been applied to some machine parts, for example, glow plugs and turbochargers of automotive engines[1]. In the case where the advanced ceramics are used as these structural parts, the low dimensional accuracy of sintered bodies requires secondary machining.

Ceramic materials has typical properties such as high hardness and low ductility. Since high hardness of the advanced ceramics makes it difficult for the cutting tool to penetrate into the workpiece, the cutting tool deteriorates rapidly due to wear and/or chipping. Cracking usually takes place when brittle materials are machined. Relatively large residual cracks induced by the cutting edge frequently cause fatal strength reduction of machined parts. Although sizes of residual cracks can be reduced by the application of lapping, polishing, horning, and superfinishing, these machining methods are rather for finishing parts having limited shapes such as plane, cylinder, and sphere. Thus, grinding with diamond wheels is the most important method in terms of machining accuracy, surface integrity, and productivity.

However, even grinding has some problems in machining of ceramic materials.

First, grinding conditions should be carefully determined. Material machining proceeds involving different removal modes such as brittle fracture and plastic flow. The material removal modes which sensitively varies depending upon grinding conditions affect not only machining accuracy and surface integrity, but also productivity.

Secondly, finishing costs are high. Abrasive utilization(i.e. grinding ratio - ground volume of material/worn volume of wheel) is usually quite poor. In addition, to achieve a good surface finish while attempting to maximizing material removal rates and resulting surface integrity, multiple step finishing approach for roughing, semi-finishing, and finishing is conventionally adopted. It is desirable to develop a fewer step roughing-finishing process suitable for producing high quality ceramic parts at high material removal rate.

Thirdly, technologies proper to grinding of hard and brittle materials should be developed: special design of grinding machine of high stiffness and high precision, effective truing and dressing of diamond wheels, automatic balancing of wheels on machine, full separation of chips from grinding fluid, complete protection from

intrusion of chips into guide planes, etc..[2]

Fourthly, recovering of deteriorated strength of ground materials should be made by removing or healing of residual cracks.[3]

This paper describes characteristics of ceramic materials and discusses principles of material removal phenomena. Then, recent techonolgies to get high quality parts and high productivity in grinding of advanced ceramics are reviewed.

2. Characteristics of Brittle Materials

High hardness of ceramic materials is caused by low density and low mobility of dislocations. These features of dislocations bring the brittleness of ceramic materials in two ways. First, stress concentration or stress singularity at the tip of a crack hardly relaxes because crack tip blunting by plastic flow is difficult to take place. Secondly, the energy required to create crack walls is mainly surface energy which is much less than the energy to be expended by the formation of plastic zone around the crack tip.

Degree of toughness of brittle materials is evaluated by fracture toughness from engineering point of view. The fracture toughness is expressed by two characteristic values which have different dimensions. One (G_c) having $J \cdot m^{-2}$ is directly derived from the energetics as the critical energy necessary to crack extension of unit area. From energy balance, this value is equal to critical strain energy release of the crack extension of unit area. The other(K_c) having $N/m^{3/2}$ is derived by the stress analysis as critical stress intensity factor in excess of which a crack extends. G_c and K_c are related by $G_c = K_c^2/E$ (in the plane stress state, where E = Young's modulus). G_c has such a merit that its physical meaning is easy to be understand, while K_c can be directly compared with the stress intensity factor derived by the stress analysis.

3. Features of Advanced Ceramics

Table 1 shows the types and properties of typical structural ceramics, Si_3N_4, SiC, Al_2O_3, and ZrO_2.[4] Since non oxide ceramics of Si_3N_4 and SiC remain strong at high temperature, they have been applied to structural parts of automotive engines and gas turbines. Si_3N_4 is more expected to be applied to structural parts than SiC because of being tougher than SiC until relatively high temperature. Fig. 1 shows ceramic parts which have been applied and are expected to be used in automotive engines[1]. Being the most stable materials in oxide ceramics

but weakening at high temperature, Al_2O_3 have been applied to chemical pump parts and valves which are used at relatively low temperature. Partial stabilized ZrO_2 (PSZ) is the toughest ceramics that are made to spend some portion of applied mechanical energy for the energy of the stress induced transformation from tetragonal phase to monoclinic phase. PSZ has been applied to cutting tools and wear resistive parts which are used at relatively low temperature.

4. Fundamentals of Material Removal Process

Material removal phenomena in machining of metals are basically understood as those of plastic flow process. As previously mentioned, material removals in machining of ceramics are, however, carried out involving both brittle fracture and plastic flow. Thus, the critical condition where the plastic flow mode transfers to brittle fracture one should be made clear in understanding the material removal phenomena of brittle material.

As the tool engages the workpiece, the compression zone is formed just beneath the contact zone of the tool, while the tensile zone exists so as to envelope the compression zone[5]. The compression zone results in forming the plastic zone under some conditions and the tensile zone provides the place where cracks begin to extend. As will be described later, cracks extend both before and after formation of plastic zone in the workpiece by the penetration of the tool[6]. There is another case that any crack does not extend even after full penetration of the tool.[7] The conditions which distinguish the three cases for the crack extension should be cleared by considering the localized stress field induced by the tool penetration. As conclusively describing, the extensity and the intensity of the localized stress field play an important role to the crack extension.

4.1 Material Removals in Cutting[7],[8]

Investigations on the orthogonal cutting process provide an important instruction in understanding the material removal phenomena in machining.

Fig. 2 shows the analytical result of the principal tensile stress distribution formed after the plastic zone in the plate workpiece fully develops by the progress of the tool with rake angle 0° . The tensile principal stress along the expected crack path has the maximum value near the plastic-elastic boundary. This tensile stress field spreads monotonously with the tool progress, while its maximum value reaches

almost constant level at early stage of the tool progress. If any crack does not extend after full development of plastic zone, plastic flow type chip can be generated like as in cutting of metals.

Since the maximum value of the tensile stress is inherent to the workpiece material, the condition whether a crack extends depends upon the extent of the tensile principal stress field. If this stress field sufficiently spreads so as to act a pre-existing crack at high stress level, the extension of the crack easily takes place. On the other hand, narrow extent of the stress field makes it difficult for the crack to extend. The extent of the stress field is determined by the depth of cut. Therefore, plastic flow type chip are formed at the depth of cut less than the critical value. On the contrary, if much larger depth of cut is adopted, brittle fracture type chip are made before full development of the plastic zone.

The critical depth of cut D_c to get plastic flow type chip is analytically given as follows.

$$D_c = \alpha (K_c/Y)^2 \qquad (1)$$

where, K_c: fracture toughness, Y: yield stress,

α: non dimensional constant independent on workpiece material (21 for the geometry in Fig. 2)

According to eq.(1), D_c's of some materials are given as follows.

Macor(machinable ceramics)	:14 μm
Glass	:0.3 μm
Al_2O_3	:1.7 μm

These values have been confirmed by the experiment.

4.2 Brittle Fracture and Plastic Flow due to Indentation, Sliding Contact, and Adrading

4.2.1 Indentation

The most basic interaction between an abrasive and a workpiece in grinding and other abradings may be due to the indentation. For simplicity, the spherical abrasive is treated in later.

Fig. 3 shows brittle fracture and plastic flow by the indentation.[9] It is well known that brittle crack whose trace has a truncated conical shape extends beneath the indenter with relatively large radius. This crack, so called "cone crack" initiates under the elastic stress state. On the other hand, by using an indenter with sufficiently small radius, plastic flow is at first induced without any

crack extension. As the penetration of the indenter proceeds, " median crack " initiates near plastic-elastic boundary and extends downward. Upon complete unloading, "lateral cracks " extends toward the workpiece surface and may accordingly lead to chipping.[10]

The facts that the cone crack extends in the elastic deformation state and plastic deformation can begin without any crack extension imply that the condition necessary to the crack extension is determined not only by the intensity of the stress field, but also by its extensity. Thus, there exists the critical indenter radius R_c.[11] By adopting indenter radius less than it, any crack does not extend at least in the elastic deformation state. When Poisson's ratios of workpieces are almost the same, R_c is proportional to $E \cdot K_{Ic}^2 \cdot H_v^3$. Table 2 shows R_c in the indentation and the sliding contact(see the next section).[11]

4.2.2 Sliding Contact

It is known that the sliding motion of the indenter plays an important role in crack extension. In the elastic contact, partial cone cracks occur as shown in Fig. 4.[6] Since the compressive stress field is formed ahead the indenter, the cracks extend from behind to side so as to eliminate the front part of the cone crack. From the comparison of R_c's shown in Table 2, it is evident that R_c substantially decreases with friction. This is because the tensile stress field behind the indenter largely develops even by small friction.

Thermal stress induced by sliding motion at high speed contributes to controlling crack extension. Fig. 5 shows the maximum principal stress distributions caused by sliding motion of two dimensional slider (cylinder).[4] The maximum thermal principal stress field in Fig. 5(b) shows negative stresses in almost the same region where the maximum mechanical principal stresses(Fig. 5(a)) are positive. This indicates that tensile stresses due to the mechanical loads are relaxed by the thermal load. The maximum combined principal stress field shown in Fig 5(c) delineates the tendency that the tensile stress is small in comparison with that in Fig. 5(a).

4.2.3 Abrading

As expected by the findings in cutting, indentation, and sliding contact, material removals in abrading occur both by plastic flow and brittle fracture. As the abrasive penetrates the workpiece, cutting action takes place by plastic flow which is followed by fracture if the penetration becomes sufficiently large. Three types of cracks are

generated: lateral cracks which lead to material removal, partial cone cracks and median cracks both of which cause strength degradation.

If the intensity and extensity of the stress field maintain below some critical level, fracture damage may be avoided or minimized. The approach to achieve this object is to adopt grain depth of cut smaller than the critical value varying with grain size.

5. Practical Grinding Process of Advanced Ceramics

5.1 Specific Grinding Energy

Attempts to evaluate the grindablity of advanced ceramics have been carried out by using hardness, fracture toughness, and other material constants or values combined by these values. As previously described, material removals by grinding take place by complex phenomena involving plastic flow and brittle fracture. Thus, the grindability is hard to be evaluated by any single value. Moreover, the measures to evaluate the grindability should be defined according to engineering aims.

Specific grinding energy U which is defined as the energy required to remove material of unit volume is one of measures to evaluate the grindability of materials. This is experimentally derived by the following equation.

$$U = F_T v/(V \Delta B) \qquad (2)$$

where, F_T: tangential grinding force, v: work speed, V: wheel speed, Δ: wheel depth of cut, B: wheel width.

Figs. 6 and 7 show the relations between the specific grinding energy and wheel depth of cut, where the advanced ceramics are ground by a diamond wheel at grinding speed 1600 m/min.[12] Apparently, the specific grinding energy is not inherent to the work material but varies with grinding conditions.

If the material removals by grinding are carried out both by plastic flow and brittle fracture, the specific grinding energy is derived as eq.(3) by considering the pressure and friction on an abrasive and the removal volume by the abrasive.[13]

$$U = f_F \cdot H_V \{1+(3\pi/2)f\sqrt{R/(2g)}\} \qquad (3)$$

where, it is assumed that the abrasive is a sphere of radius R and energy for the brittle fracture is negligibly small compared to that for the plastic flow.

f_P: fraction of removal volume by plastic flow in total removal volume,

H_V: Vicker's hardness,

f: frictional coefficient between the abrasive and the workpiece,

g: grain depth of cut.

The above equation implies that the specific grinding energy increases with increase of the fraction of volume removed by plastic flow, f_P.

The value of f_P is reasonably given by a/Cl in considering that a groove is removed by plastic flow and the rest by brittle fracture (lateral cracking) in Fig. 8.[10] Sizes of the lateral crack are experimentally given in Fig. 9.[10] Therefore, the experimental equation expressing a/Cl is given as follows.[14]

$$a/Cl = A(m)\{K_c \phi/(H_V\sqrt{a})\}^m \qquad (4)$$

where, $\phi = H_V/Y$, Y: yield stress, $\phi \fallingdotseq 3$

$Cl/a \geq 3$ $\quad m = 1,$ $\quad A(1) = 5$

$Cl/a = 1$ $\quad m = 0,$ $\quad A(0) = 1$

$1 < Cl/a < 3$ $\quad 0 < m < 1,$ $\quad 1 < A(m) < 5$.

By using the relation, $f_P = a/Cl$, the material constant term in eq.(4) is expressed by $K_c^m H_V^{1-m}$. The value, m, may have a meaning of brittleness index in material removal. Consequently,

By perfect plastic flow : $m = 0$, U is proportional to H_V,

By perfect brittle fracture: $m = 1$, U is proportional to K_c,

By combined removal : $0 < m < 1$, U is proportional to $K_c^m H_V^{1-m}$

Since m varies with grinding conditions, the above relation indicates that the specific grinding energy largely varies for a material and even its order among materials changes (higher H_V or Higher K_c does not always cause higher U).[14] It have been confirmed that the above relation can be basically applied to superfinishing and horning.

5.2 Strength of Ground Workpiece

The median crack may be the most dangerous to cause strength deterioration of ground ceramics. If its size is known, its strength may be evaluated. Unfortunately, its size is difficult to be analytically related with abrading conditions. So, its size should be inevitably estimated by analogy with indentation crack.

5.2.1 Crack Extension Length in Indentation

Fig. 10 shows the principal stress distribution caused by the elasto-plastic indentation(material: glass, σ_1: the maximum principal stress, p_m: mean contact pressure, a: half radius of contact zone, R: radius of indenter).[15] The stress contributing to its extension is high tensile principal stress which occurs in the vicinity of the plastic-elastic boundary apart from the contact zone. Fig.11 shows the crack extension length (radius of extended disk-type crack) versus the indenter radius.[15] Since the intensity of the stress field is the same at a a/R, the results shown in this figure indicate that the crack extension size increases not only with the intensity of the stress field, but also with its extensity.

5.2.2 Grain Depth of Cut in Grinding

In order to know how intensively and extensively an abrasive grain acts on the work material in grinding, the grain depth of cut should, at least, be evaluated. However, its evaluation is known to be obscure or laborious if it is exactly treated. Recently, a new simple method has been proposed measuring the distribution of grains on the working surface of practical grinding wheel at first and then statistically analyzing effective and noneffective action of abrasive grains.[16] According to the method, the rigidity of abrasive binder can be taken into account in the analysis. Only the measurement of the grain distribution on the working surface is introduced here as the first stage of the method.

The working surface of a grinding wheel is pressed against a brass surface polished mirror finish and rotated over a constant distance in the circumferential direction of the grinding wheel. Then, intervals of successive grains are measured by using the profile of a transferred scratch(see schematic diagram in Fig. 12). The interval of successive grains s is defined by the following equation which depends on radius depth δ from the outermost circumference of the grinding wheel.[16]

$$s(\delta) = l \cdot B / \Sigma b_i(\delta) \qquad (5)$$

where, l: grinding wheel transfer distance, B: grinding wheel width,
b_i: removal width removed by a grain located at the point apart by radius depth δ from the outermost of the grinding wheel.

Fig.13 shows simulation result for mean value of effective maximum

grain depth of cut in using wheels listed in Table 3[16]. It is found that metal-bonded grinding wheels have higher values than resinoid-bonded grinding wheels. This is because the rigidity of grinding wheel bonding materials has a strong influence.

5.2.3 Influence of Grinding Conditions on Strength of Ground Ceramics

Fig.14 shows results of bending tests of ground Si_3N_4.[17] It is evident that the strength decreases considerably with increase in the grain size of the grinding wheel. The strength is also affected by grinding direction. When the specimen is ground perpendicular to the grinding direction, strength decrease becomes at higher degree.

Fig.15 shows results of fracture strength of ground Si_3N_4 versus (mean value of effective maximum) grain depth of cut.[18] The results indicate that the fracture strength considerably decreases in the range of grain depth of cut larger than 0.5 to 1.0 μm but has the level of polished workpiece in its range smaller than 0.1μm. It is also shown that the fracture strength degradation of the workpiece ground by finer grain does not occur until higher grain depth of cut.

5.3 Residual Stress in Ground Surface Layer

Fig. 16 shows the residual stress distributions in the depth direction, where measurement by X-ray diffraction is successively applied after each removal of surface layer.[19] As seen in this figure, the residual stress in ground surface layer of ceramic materials are generally compressive, while they become tensile or compressive depending upon grinding conditions. This compressive stress is of advantage to the strength of ground ceramics. The reason that ZrO_2 has large compressive residual stress is due to the stress induced phase transformation.

6. Modern Technologies of Grinding of Advanced Ceramics

6.1 Grinding Machine[2]

As described above, material removal modes in grinding of ceramics vary fairly depending upon grain depth of cut. In addition, advanced ceramics generally have high degree of hardness. Thus, the grinding machine of high stiffness and high precision should be prepared. Furthermore, complete protection from intrusion of chips into guide planes should be made. For these purposes, hydrostatic oil or air bearing and slide are used. To reduce the vibration induced by imbalance of mass of the wheel, automatic balancing of wheel is carried out in

process by injecting some amount of fluid into pockets equipped in the wheel spindle. Built-in motor is also applied to wheel spindle system to eliminate vibration due to the deviation between axes of the spindle andthe motor. Full separation of chips from grinding fluid is needed.

6.2 Truing and Dressing

Truing and dressing of super abrasive wheels are cumbersome because their abrasives are tightly bonded by resinoid or metal. Diamond truer and conventional grain dresser have been applied. Recently, electrolytic in process dressing method has been developed for metal bonded super abrasive wheel.[20] By using solution type grinding fluid with weak conductivity, the electrolytic removal of the binder makes the cutting edge of grain stuck out in process. Since stable cutting edges of grain is obtained by the method, mirror surface grinding of advanced ceramics can be achieved.

6.3 High Speed, Low Damage Grinding of Advanced Ceramics

In the manufacture of structural ceramic parts, it is known that the finishing costs can comprise up to 80% of the entire manufacturing cost. Generally, these finishing processes utilize diamond grinding wheels which typically account for 50% to 70% of the finishing costs.

Grinding cost of material removals of unit volume C_G is expressed by the following equation.[2]

$$C_G = C_L/(v \Delta B) + C_W / G \qquad (6)$$

where, C_L: labor cost and machine cost / time, G: grinding ratio
C_W: wheel cost / wheel volume

Table 4 shows grinding costs of Si_3N_4 for provided grinding ratios.[2] The results mean that the strategy to reduce the grinding cost is to elevate grinding rate because the fraction of wheel cost is considerably low in the total cost.

The way to get high grinding rates while maintaining a small grain depth of cut is through the use of high wheel speeds and fine abrasive wheels. Since small grain depth of cut requires high specific grinding energy, considerably high grinding temperature rise occurs being enhanced by the effect of high wheel speed. As described previously, elevated grinding zone temperatures tend to inhibit fracture and promote the plastic flow type grinding[4]. High temperatures can have a beneficial effect on the resulting surface integrity, which is contrary

to the caseof grinding metals.

Fig.17 shows bending strength of Si_3N_4 ground by normal surface grinding and high-speed and speed-stroke grinding, where the grinding conditions are as shown in Table 5.[21] The reason that the bending strength of the workpiece ground by high speed and speed stroke grinding maintains high value even at high stock removal rate is due to low grain depth cut as shown in Fig.18. Thus, these results indicate that the high speed, low damage grinding was achieved.

6.4 Crack Healing with Laser Irradiation in Si_3N_4[3]

Healing of minute cracks in the surface layer of advanced ceramics is one of important technology for practical use. The healing method for Si_3N_4 have been proposed being based on heating with pulsed YAG laser irradiation. Laser heating for 20 seconds in atmosphere of nitrogen gas elevates the surface temperature up to 1600 - 1750 ℃. Fig.19 shows flexural strength of ground specimen after laser heating. It is evident that the method is useful for recovering the strength. The healing by laser irradiation is considered to be caused by resintering with the sintering aids and by boundary consolidation with crystallization silicon nitride-yittrium oxide.

7. Conclusive Remarks

Modern technologies introduced here in machining of advanced ceramics promote their application to various structural parts. Recently, various compound grinding methods such as electro mechanical compound grinding, electro-chemical grinding, compound micro wave grinding, compound laser beam grinding, compound electrolytic plasma grinding have been proposed. They should be paid attention.

References

(1) H.Kawamoto et al.;Application of Ceramic Parts to Engines, Uchidarokakuho,1990,p.1,(in Japanese)

(2) K.Okano,M.Ishiyama,Y.Niino;Fine Ceramics,Ass.Tec.Inv.Fine Cer., p.1598,(in Japanese).

(3) Y.Kishimoto,M.Watanabe;J.JSPE,59(1993)833.

(4) Y.Tanaka,T.Nishioka,G.H.Park;

(5) F.C.Frank,B.R.Lawn;Proc.Roy.Soc.(London),Ser.A,299(1967)291

(6) B.R.Lawn,A.G.Evans;J.Mat.Sci.,12(1977)2195.

(7) K.Mizutani,Y.Tanaka;J.JSPE,52(1986)1768.

(8) K.Mizutani,Y.Tanaka;J.JSPE,53(1987)1758.

(9) S.S.Ching, C.B.Marshall, A.G.Evans; J.Appl.Phys., 53(1), (1982)298.
(10) A.G.Evans, T.R.Wilshaw; Acta Meta., 24(1976)939.
(11) Y.Tanaka, G.H.Park; J.Soc.Mat.Sci., Japan, 41(1992)260.
(12) Y.Tanaka, K.Mizutani, G.H.Park; Japan Korea Ceramic Seminar (1989)
(13) Y.Tanaka, M.Ido, H.Matsuo; Proc.JSPE, Spring, (1981), p.260.
(14) Y.Tanaka; New Ceramics, 1(1988)37.
(15) Y.Tanaka, T.Nishikawa; Proc.2nd Mat.Pro.Conf., No.940 36(1994)144.
(16) T.Nishioka, Y.Tanaka, A.Yamakawa, M.Miyake; J.Cer.Soc.Japan, 102(1994)928.
(17) M.Ito; Fine Ceramics Technologies, Kogyochosakai Press, p.219, (in Japanese)
(18) T.Nishioka, Y.Tanaka, A.Yamakawa, M.Miyake; J.Cer.Soc.Japan, 103(1995)335.
(19) K.Murata, K.Mizutani, Y.Tanaka; J.Mat.Sci.Japan, 41(1992)
(20) H.Omori, T.Nakagawa; J.JSGE, 34(1990)14.
(21) T.NIshioka, Y.Ito, T.Yamamoto, A.Yamakawa, M.Miyake, Y.Tanaka; Proc.JSPE, Kansai Dist., 1995, submitted.

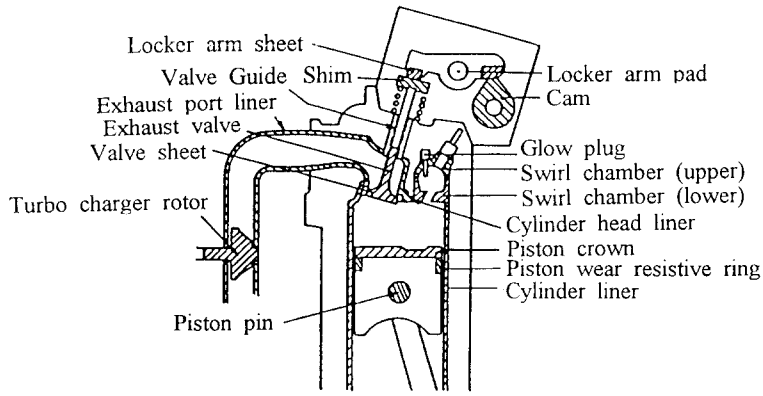

Fig. 1 Ceramic parts for automotive engine

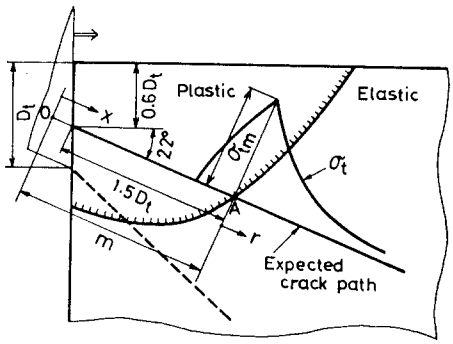

Fig. 2 Plastic zone, crack path, and distribution of the maximum principal stress on the path

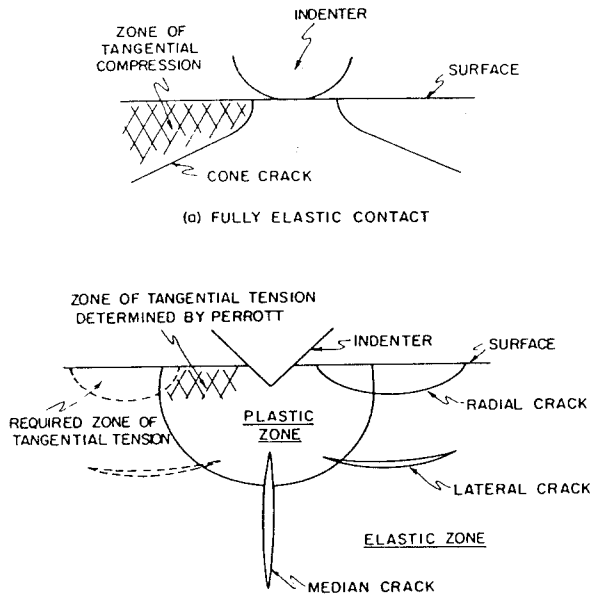

Fig. 3 Schematic indicating the different morphologies that develop for fully elastic and elastic/plastic contact

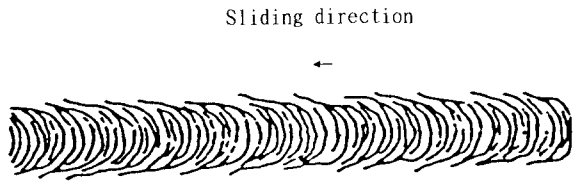

Fig. 4 Partial cone crack induced by sliding of a sphere on the surface of brittle material

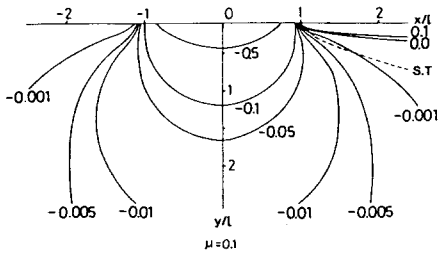

Stress : σ_1/p_e
(a) By mechanical loads.

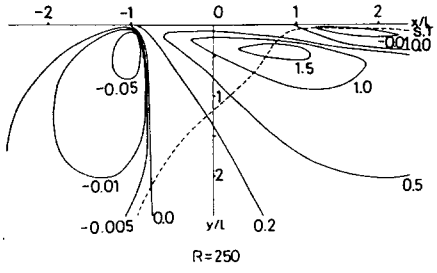

Stress : $\sigma_1/(\mu \cdot \theta \cdot m \cdot p_e)$
(b) By thermal load.

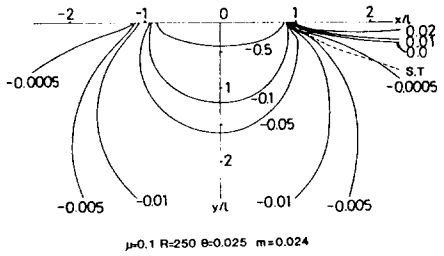

Stress : σ_1/p_e
(c) By combined load.

Fig. 5 Maximum principal stress fields induced by sliding of a cylinder on the glass surface

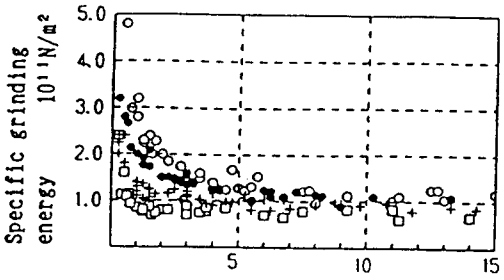

Fig. 6 Wheel depth of cut μm
Specific grinding energy (#140 wheel)
Work material : Si_3N_4
v(m/min)= ○:2.5, ●:5, +:10, □:20

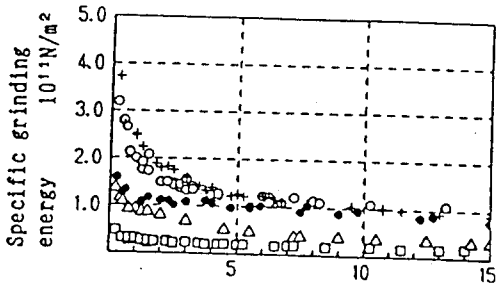

Fig. 7 Wheel depth of cut μm
Specific grinding energy (#140 wheel)
○:Si_3N_4, ●:SiC, +:ZrO_2, □:Al_2O_3, △:Glass

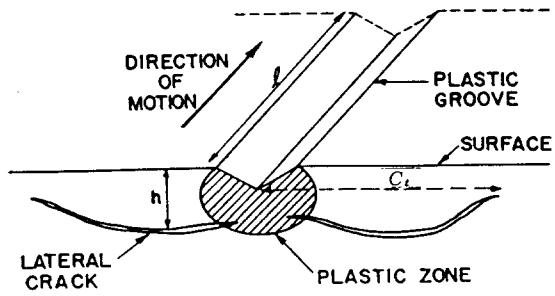

Fig. 8 A schematic indicating the mature of the lateral cracking that leads to material removal

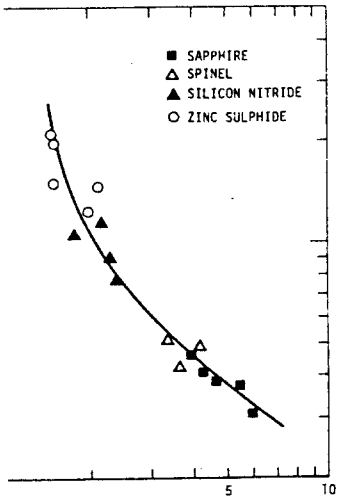

ɔrmalized crack length Cl as a
the normalized fracture
r lateral cracks

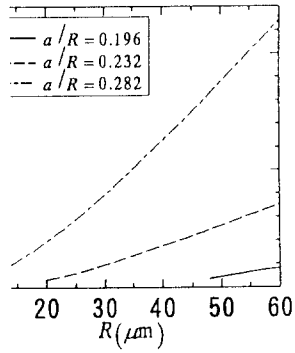

ɪsion length (radius) c vs. indenter radius

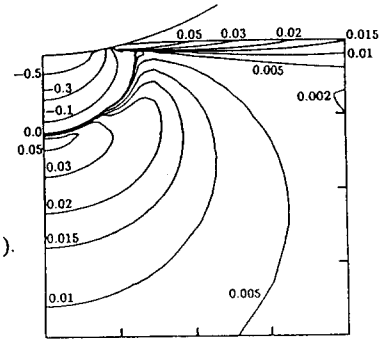

$(a/R = 0.282)$.

Fig. 10 Contour of normalized principal stress σ_1/p_m

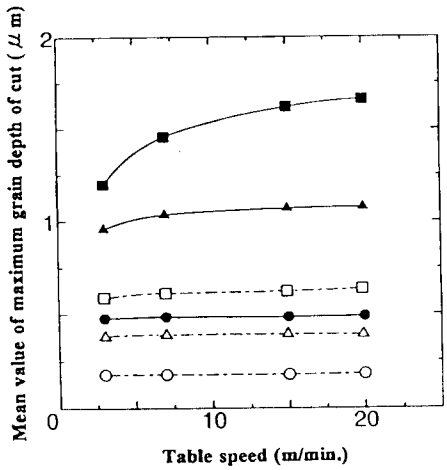

Fig. 13 Simulation result for mean value of effective maximum grain depth of cut.
Wheel depth of cut;
Resinoid-bonded wheel : □ 10μm, △ 6.5μm, ○ 3μm.
Metal-bonded wheel : ■ 10μm, ▲ 6.5μm, ● 3μm.

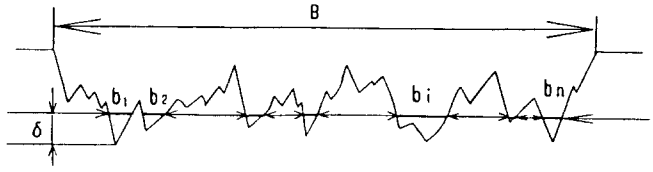

Fig. 12 Model profile of transcript of work-surface of grinding wheel onto brass.
B: Width of grinding wheel, b_i: Length of passing traces of cutting edges, δ: Radial depth of grinding wheel.

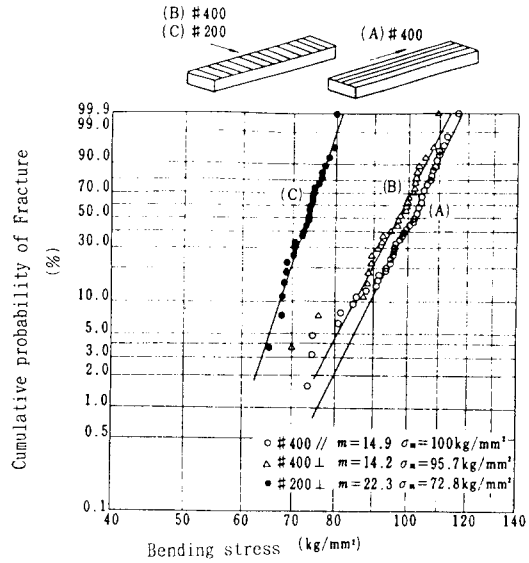

Fig. 14 Influence of grinding directions and abrasive grain sizes on bending strength

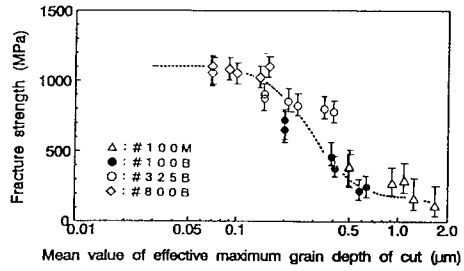

Fig. 15 The relation between strength degradation of Si_3N_4 work piece and mean value of effective maximum grain depth of cut. B : Resinoid-bonded wheel, M : Metal-bonded wheel, Grain size : #100=125-150 μm, #325=37-45 μm, #800=12-25 μm.

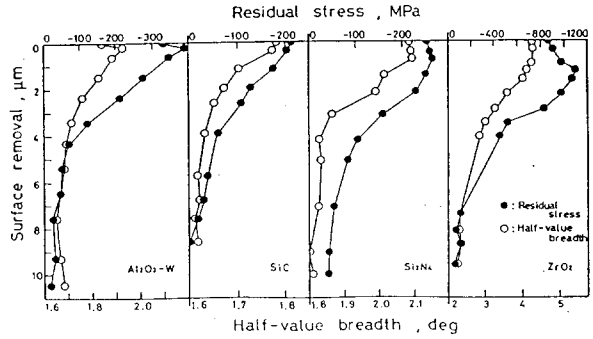

Fig. 16 Changes in the residual stress and the half-value breadth of diffraction profile for the specimens stepwise removed its surfaces

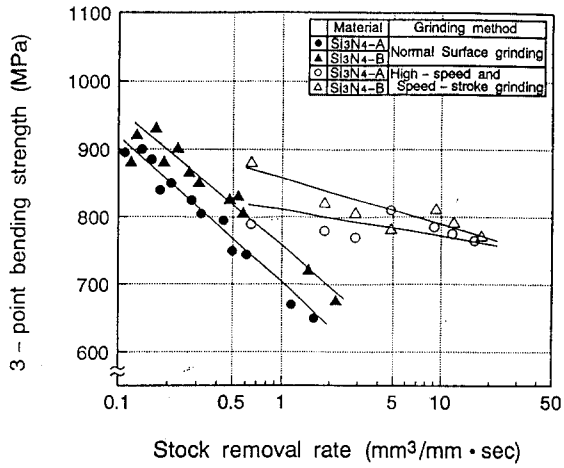

Fig. 17 The relationship between stock removal rate and 3-point bending strength of ground workpiece

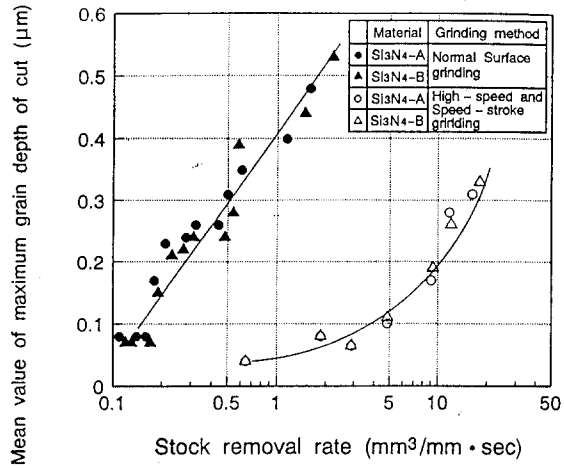

Fig. 18 The relationship between stock removal rate and mean value of maximum grain depth of cut

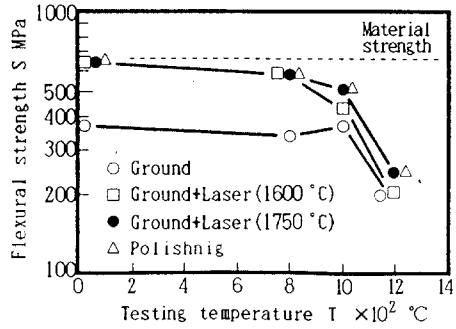

Fig. 19 Flexural strength of ground specimen after laser heating

Table.1 Properties of Advances Ceramics

	Si_3N_4	SiC	Glass	Al_2O_3	ZrO_2
Poisson ratio ν	0.25	0.15	0.24	0.23	0.3
Young's modulus E $[10^9\ N/m^2]$	304	402	70.0	353	206
Hardness Hv $[10^9\ N/m^2]$	14.7	24.5	5.4	15.7	12.7
Fracture toughness K_{IC}	4.0	4.0	0.7	4.0	8.0
K_{ICS}	2.2	2.0	0.3	1.7	–

K_{IC} for macro crack
K_{ICS} for micro crack

Table.2 Critical Radius of Indenter (μm)

μ		Si_3N_4	SiC	Glass	Al_2O_3	ZrO_2
0.0	K_{IC}	880	103	141	666	8180
	K_{ICS}	266	26	26	120	--
0.1	K_{IC}	200	36	34	171	1490
	K_{ICS}	60	9	6	31	--

Table 3

Resinoid-bonded wheel	SD100, 75 (Grain:EBG made by General Electric)
Metal-bonded wheel	SD100, 75 (Grain:MBG-660T made by General Electric)

Table 4 Cost comparison for Si_3N_4 Grinding[2,3]

Depth of Cut (μm/pass)	10	20	30	40
Grinding ratio	760	530	380	270
Cost of Grinding Wheel For 1cm³ removal of Si_3N_4[1] (Yen)	5.3	7.5	10.5	14.8
Other Cost for 1cm³ removal of Si_3N_4[2] (Yen)	1,600	800	530	400

1)Price of Grinding Wheel: 4,000Yen/cm³
2)Other Costs including Labor Cost: 5,000Yen/hour
Calculated from time for plunge grinding

Table 5 The conditions of normal test grinding and high-speed and speed-stroke test grinding

Grinding method	Wheel speed (m/sec.)	Table speed (m/min.)	Wheel depth of cut (μm)
Normal grinding	25.0	3, 10, 20	3, 6.5, 15, 30
High-speed and speed-stroke grinding	55.0	45	0.9, 2.5
		70	2.5, 4.2, 8.4
		90	8.4, 12.5